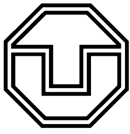

TECHNISCHE UNIVERSITÄT DRESDEN

Faculty of Electrical and Computer Engineering, Institute of Power Engineering, Chair of Power Electronics

Filsecker, F.; Alvarez, R.; Bernet, S., "The Investigation of a 6.5-kV, 1-kA SiC Diode Module for Medium Voltage Converters," Power Electronics, IEEE Transactions on, vol.29, no.5, pp.2272-2280, May 2014

This paper is published by the authors in its *accepted* version on the homepage of the Chair of Power Electronics of the Technische Universität Dresden:

http://tu-dresden.de/et/le

The *final, published article* can be found on the IEEE Xplore database:

http://dx.doi.org/10.1109/TPEL.2013.2278190

© 2013 IEEE. Personal use of this material is permitted. Permission from IEEE must be obtained for all other uses, in any current or future media, including reprinting / republishing this material for advertising or promotional purposes, creating new collective works, for resale or redistribution to servers or lists, or reuse of any Copyrighted component of this work in other works.

Investigation of a 6.5-kV, 1-kA SiC Diode Module for Medium Voltage Converters

Felipe Filsecker, Rodrigo Alvarez, Steffen Bernet

Abstract—**This paper introduces a 6.5-kV 1-kA SiC PiN diode module for megawatt-range medium voltage converters. The analysis comprises a short description of the die and module technology and a device characterization. The effects of di/dt and temperature variation, as well as parasitic oscillations are discussed. A comparison of the results with a commercial Si diode (6.5 kV and 1.2 kA) is included. In the last section, an estimation of maximum converter output power, maximum switching frequency, losses and efficiency in a 3L-NPC converter operating with SiC and Si diodes is presented. The analyzed diode module exhibits a very good performance regarding switching loss reduction, which allows an increase of at least 16% in the output power of a 6-MVA converter. Alternatively, the switching frequency can be increased in 46%.**

Index Terms—**SiC diode, device characterization, medium voltage converter, NPC, comparison.**

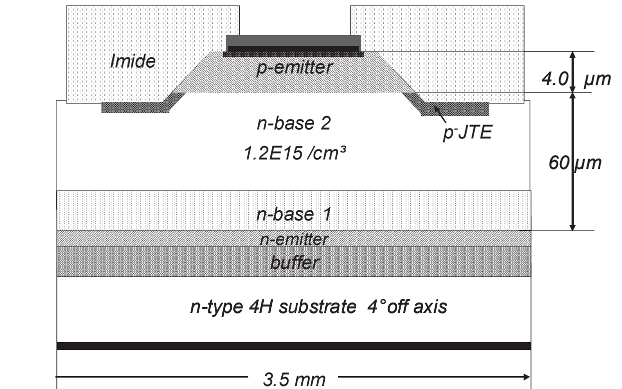

Fig. 1. SiC diode chip design cross section. [16]

I. Introduction

Medium voltage converters (MVC) are essential for power generation and distribution systems, industrial drives and traction systems. Their limitations are mainly determined by the power semiconductors used. Silicon devices exhibit a trade-off between conduction and switching losses. Therefore, for a given device structure and blocking capability, it is not possible to optimize a device for minimal conduction and switching losses simultaneously. [1]

Loss reduction is not the only aim in power semiconductor development. Features like higher power density capability – e.g. higher blocking voltages, high temperature operation, wide safe operating area (SOA) –, ruggedness and reliability are also demanded. The maturity of silicon devices makes a major breakthrough improbable. Hence, new wide band gap semiconductors, due to their superior physical properties, have become attractive for new developments in power electronics, including the field of MVC. [1], [2]

MVCs would drastically profit from the application of SiC power devices, especially from the loss reduction in the power devices, extended SOA, operation at higher junction temperatures and voltages. Since the maximum die size and its maximal current are limited by the wafer production technology, modules with high current ratings can only be achieved through parallel connection of many dies. As a consequence, a proper packaging becomes one of the crucial barriers to overcome. Problems such as heat distribution, parasitic inductances, thermal stability at high temperatures, among others, need to be solved. Reliability issues are also a decisive factor before reaching commercial status. [3]–[5]

The increasing number of papers on this topic show the interest in power semiconductors based on SiC for industrial applications. Several high voltage devices targeting high power applications have been reported, either as chip [6]–[8] or module [9]–[13]. This paper presents an overview of a SiC diode module rated for 6.5 kV and 1000 A, which comprises device characterization, comparison with a Si diode and converter loss estimation. Detailed information can be found in [14] for the diode module characterization and in [15] for the module comparison. The SiC diode chip and module development have been described in [16], [17].

II. Diode chip and module

SiC diode module prototypes capable of handling voltages over 4 kV and currents of at least 400 A are still in an early development stage. In [13], a 4.5 kV, 1000 A diode capable of withstanding up to 300°C is introduced. Another approach to module design is made in [9]: A hybrid module IEGT/SiC PiN diode rated for 4.5 kV and 400 A is used in a 2.75 kV, 1 MVA inverter.

The basic structure of the diodes used in the module studied here is shown in Fig. 1. Each die has a size of $3.5\times3.5\,mm^2$ with an anode area of $7.1\,mm^2$ [16]. The module design uses the same packaging of commercial 6.5-kV Si diode modules with dimensions of $130\times140\times48\,mm^3$. The nominal values of the diode module are comparable to those of the Si diode DD600S65K1 used in the comparison: 6.5 kV, 2×500 A (SiC) vs. 6.5 kV, 2×600 A (Si). Both SiC and Si diode modules consist of two diode systems that can be used independently or connected in parallel, which means that the full SiC diode module can handle currents of 1 kA.

Inside the SiC diode module there are 4 DCB substrates, each with 20 SiC diode chips. With 80 SiC chips per module,

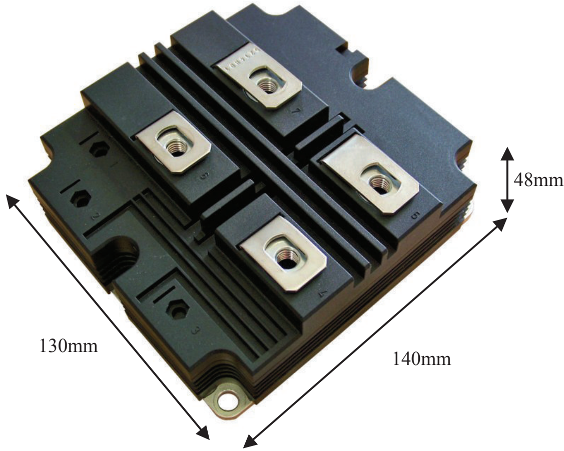

Fig. 2. 6.5-kV, 1-kA SiC diode module.

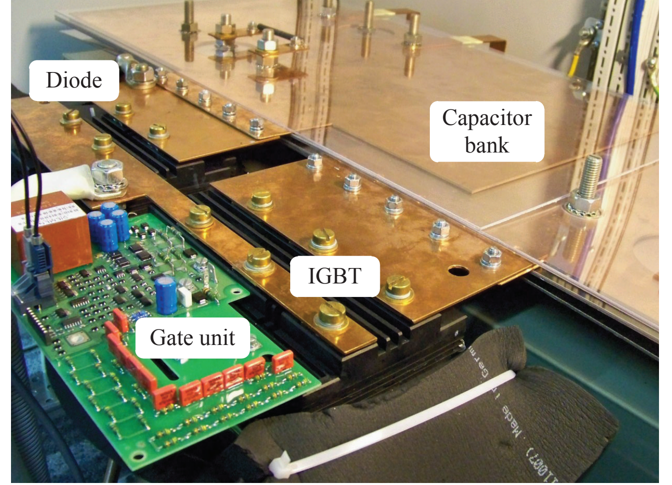

(a)

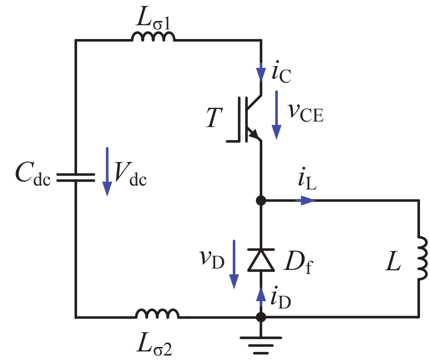

(b)

Fig. 3. Test bench (a) experimental setup photo, (b) schematic diagram of test circuit (T FZ600R65KF2, C_{dc} = 2 mF, $L_{\sigma 1+2}$ = 235 nH, L = 1 mH).

TABLE I
SIC AND SI DIODE MODULE PARAMETERS

Type / model	SiC prototype	Si DD600S65K1
Voltage (V)	6500	6500
Current (A)	1000	1200
Module size (mm^3)	130×140×48	130×140×48
Number of dies	80	24
Die active area (mm^2)	7.1	84.6
Module act. area (cm^2)	5.7	20.3
$R_{th,jc}$ (K/kW)	13.9	10.5
$R_{th,ch}$ (K/kW)	9.9	8.0

the total active area amounts to 5.68 cm^2 [16], [17]. The diode module DD600S65K1 chosen for the comparison contains 24 Si chips with an active area of 84.6 mm^2 each, totalizing an active area of 20.3 cm^2 per module. For the results shown in the paper, full Si and SiC modules were used (both anode-cathode pairs connected in parallel). Even though the module size is the same, the difference in the active area available in both modules has a ratio of 1:4. This affects the performance of the SiC diode negatively, especially when considering heat dissipation, but it also reflects the current development stage of SiC devices, where the die size is limited by wafer defects. The information regarding the modules is summarized in Tab. I.

One of the critical issues in SiC diode chip design is the problem of forward degradation, which needs to be solved in order to get a better yield and lower the costs. It originates in existing substrate crystal defects in SiC, which have a direct effect in the degradation of the forward characteristic, reducing the active area of the chip and, thus, increasing the on-state voltage [18]. Cost is a major issue in SiC semiconductor manufacturing; it will stay high as long as no appropriate technique enables a production of defect-free wafers in a large quantity [19].

In module design, ways of reducing peaks in the electrical field distribution are sought, including adequate passivation methods and optimized substrate technologies [20]. The new challenges of an extended temperature range (>150°C) are also part of ongoing investigations [21], [22].

III. Device characterization and comparison

A. Test bench setup

The test circuit is a buck converter, which allows the study of the switching behavior of an active switch T and its corresponding freewheeling diode D_f through the use of a double-pulse switching pattern, see Fig. 3b.

A robust mechanical design was accomplished using 2 mm-thick planar busbars connecting the dc-link capacitor C_{dc} (composed of two 1 mF capacitors in parallel) and the modules, see Fig. 3a. This design allows to keep the stray inductance low, which is necessary for hard switched devices. The load L is an air-core inductor of 1 mH. The stray inductance of the commutation circuit (C_{dc}, T, D_f) has a value of 235 nH. For simplicity, this inductance is represented by two concentrated inductors $L_{\sigma 1}$, $L_{\sigma 2}$ in Fig. 3b.

The junction temperature of the devices is controlled in a closed-loop by a heating/cooling device, which sets the temperature of the liquid that flows through the plate where the modules are attached to. The dc-link capacitor is charged by a high voltage power supply before the measurements are carried out. A partially automated measurement system was used. The values of V_{dc} and I_L are set using a LabVIEW program on a PC connected to the test bench. The measurements are captured

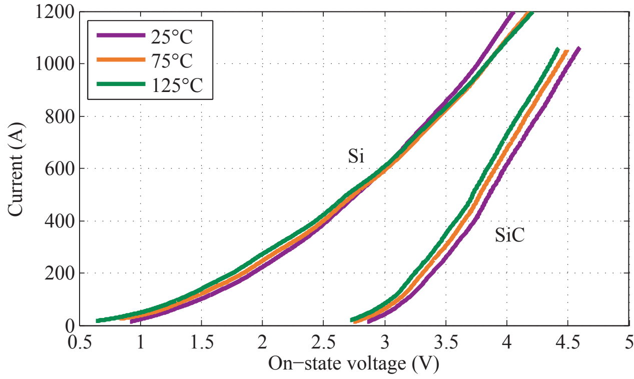

Fig. 4. Diode on-state voltage at 25, 75 and 125°C, Si: diode DD600S65K1 (full module), SiC: SiC diode, 80 chips in parallel.

by one 8-bit, four-channel, 200-MHz digital oscilloscope.

Regarding the measurements for the on-state voltage, these were conducted using the same circuit presented in Fig. 3b. The voltage probe was changed to one with lower attenuation and the load inductance was reduced to L = 58 µH. Instead of a double-pulse, a single-pulse measurement was used. The decaying current ramp through the diode during the free-wheeling phase after the IGBT turn-off was captured together with the voltage waveform.

The switch T used in the test is a 6.5-kV IGBT from Infineon, model FZ600R65KF2, with a nominal current rating of 600 A. It is operated with an industrial gate unit that has an output power of 3.5 W and a gate voltages of -10 V and +15 V.

B. Static behavior

Fig. 4 shows the measured forward characteristic for the SiC diode as well as for the Si diode DD600S65K1 at temperatures of 25, 75 and 125°C. The forward voltage at 600 A and 25°C is 2.99 V for the Si diode and 3.98 V for the SiC diode. At 125°C the Si diode has 2.98 V and the SiC diode 3.84 V.

The Si diode shows a positive temperature coefficient for high currents, which is favorable for the thermal stability of parallel connected chips. On the other side, the SiC diode exhibits a negative temperature coefficient of approximately -1.4 mV/K, which is in accordance to previous measurements done to single diode chips [16]. No thermal runaway was observed after conducting tests under continuous load conditions (100 A/cm^2 dc, 2 h long). The average temperature variation in the measured chips was less than –1 K, with a maximum increase of 7 K in one chip. After 90 min the temperature remained stable.

As the results indicate, the on-state voltage of SiC diodes is still high when compared with the Si counterpart, see Fig. 4. This is mainly due to the high threshold voltage in SiC diodes and the higher current density used in the SiC diode module. Larger die size and/or an increase in the paralleled dies would minimize this drawback.

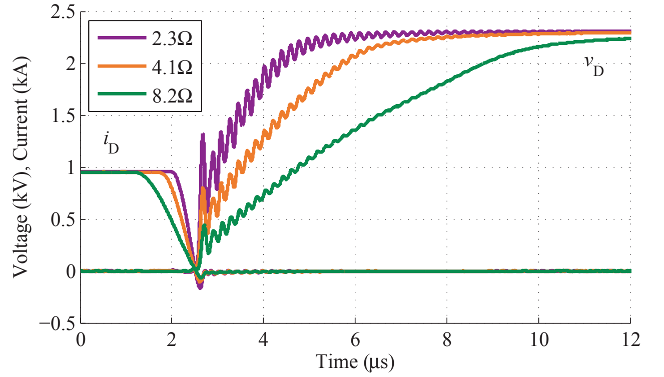

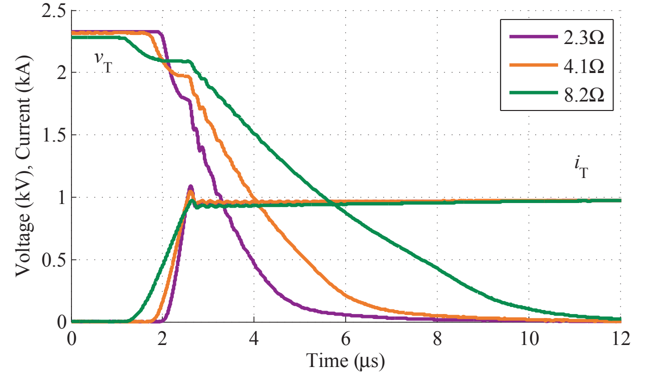

Fig. 5. Commutation waveforms for different $R_{G,on}$ values, up: diode turn-off transient, down: IGBT turn-on transient (V_{dc} = 2.4 kV, I_D = 1000 A, T_j = 25°C, L_σ = 235 nH).

C. Switching behavior

The switching behavior of the new SiC diode module was investigated. For this purpose, currents between 50 and 1000 A at dc-link voltages of 2.4, 3.0 and 3.6 kV were switched. The average junction temperatures T_j tested were 25, 75 and 125°C.

The diode turn-off and the IGBT turn-on transients show the advantages of SiC technology in loss reduction, see Fig. 5 for the influence of current change rate (di/dt) and Fig. 7 for junction temperature. Switching loss calculations for the two cases through the entire current range are presented in Figs. 6 and 8.

In Fig. 5, the different di/dt values were accomplished by changing the IGBT's gate unit turn-on resistance between 8.2, 4.1 and 2.3 Ω, that is, a di/dt variation between 0.9, 1.5 and 2.2 kA/µs at 1000 A and 25°C. The SiC diode clearly shows a small reverse recovery peak, 168A at 2.2 kA/µs and 66 A at 0.9 kA/µs.

The reverse recovery charge is also low, which has a direct influence in the reduction of losses during diode turn-off and IGBT turn-on. This can be further appreciated in Fig. 6. In the case of the diode, the switching losses remain under 14 mJ, even for high di/dt values. In the case of the IGBT, for a change of the di/dt from 0.9 to 2.1 kA/µs, IGBT turn-on losses decreased from 7.5 J to 2.3 J (I_D = 1000 A).

In contrast to 6.5-kV Si diodes, where the diode SOA determines the minimal turn-on gate resistance, the drastically

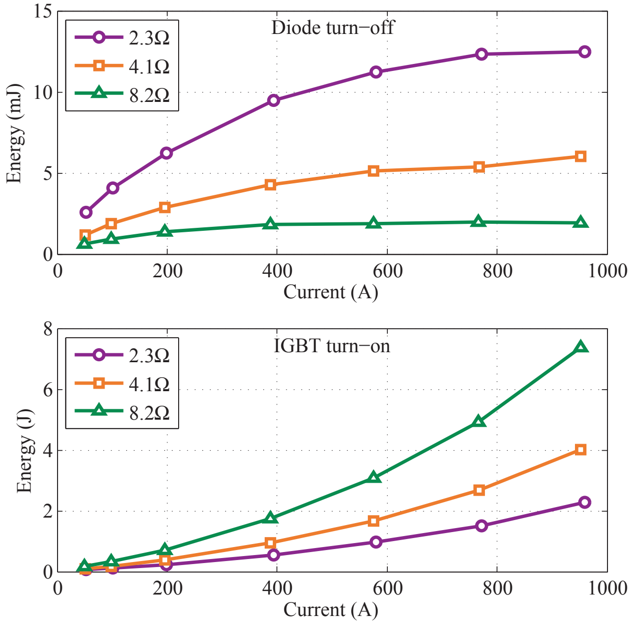

Fig. 6. Switching losses for for different $R_{\mathrm{G,on}}$ values (V_{dc} = 2.4 kV, T_{j} = 25°C, I_{D} = 50…1000 A, L_{σ} = 235 nH).

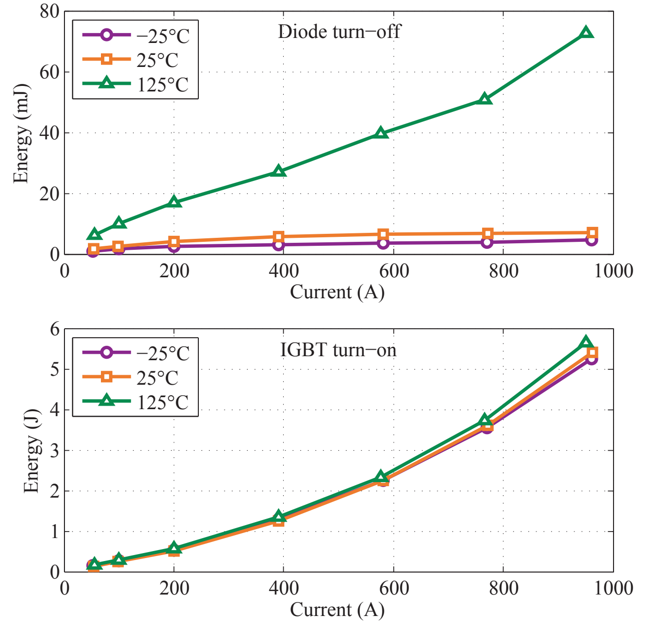

Fig. 8. Switching losses for for different T_{j} values (V_{dc} = 3 kV, $R_{\mathrm{G,on}}$ = 4.1 Ω, I_{D} = 50…1000 A, L_{σ} = 235 nH).

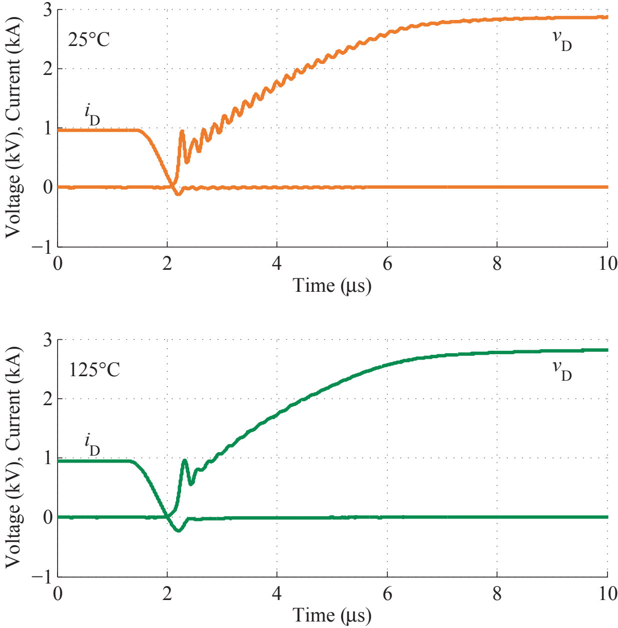

Fig. 7. Diode turn-off transient waveforms for T_{j} = 25 and 125°C (V_{dc} = 3 kV, $R_{\mathrm{G,on}}$ = 4.1 Ω, I_{D} = 1000 A, L_{σ} = 235 nH).

extended SOA of the 6.5-kV SiC diode enables a selection of a lower turn-on gate resistance to minimize the switching losses of the IGBT. However, there is one drawback to this approach, which can be seen in Fig. 7. Ringing is present in the device voltage waveforms. This is a key issue in the application of SiC devices and has been discussed in some papers, e.g. [3], [23].

For this particular diode, this problematic is analyzed in [24]. The source of the oscillations is the high di/dt after the reverse recovery maximum; the stray inductance and the device output capacitance start to resonate. As Fig. 7 shows, the oscillations are smaller at higher temperatures, due to the lower di/dt in the reverse recovery process. The fact that diode ringing due to snappiness is more critical at low rather than high temperatures has already been reported in the literature, e.g. [25]. An RC snubber connected in parallel to the diode achieved good results in dampening the oscillations [24].

Fig. 7 shows that switching at T_{j} = 125°C not only influences the oscillations but also increases losses in the diode. For 1 kA this means turn-off losses of 7 mJ at 25°C and 73 mJ at 125°C. Compared to the switching losses in the IGBT (around 5.4 J), the SiC diode turn-off losses are negligible.

Usually, the diode turn-on behavior is not regarded as critical, since stress and losses in the semiconductor are considerably lower than during turn-off. The turn-on losses in the SiC diode module are in the same order of magnitude as the turn-off losses. The low value of the forward recovery has also a positive effect by diminishing the voltage stress on the IGBT during turn-off, which has to bear the overvoltage caused by the stray inductance L_{σ} and the forward recovery voltage simultaneously. [14]

D. Si diode switching comparison

As a benchmark for 6.5-kV diode technology, the Si diode DD600S65K1 was investigated under identical conditions. Fig. 9 shows an example of the turn-off transient at 3 kV and 1 kA for T_{j} = 25 and 125°C, with a di/dt of approximately 1.5 kA/µs. The advantages of the SiC diode regarding turn-off losses are evident.

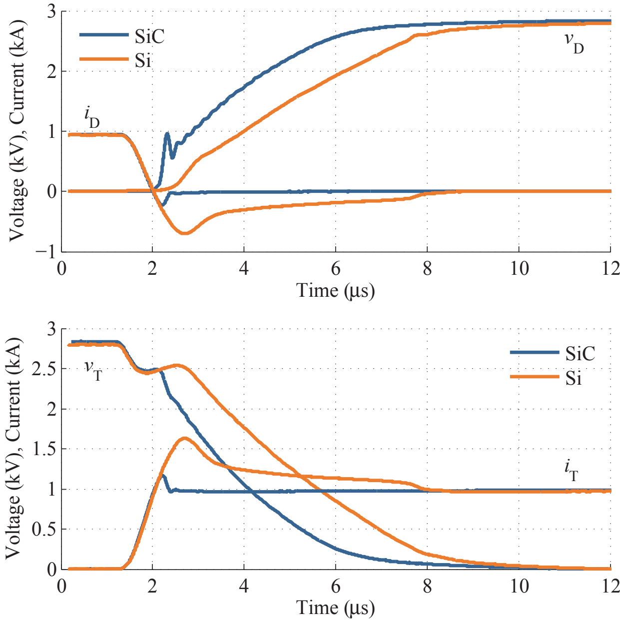

Fig. 9. Commutation waveforms at V_{dc} = 3 kV, I_D = 1 kA, di/dt = 1.8 kA/μs at T_j = 25°C and 1.6 kA/μs at 125°C, IGBT FZ600R65KF2 and Si diode DD600S65K1. Up: diode turn-off, down: IGBT turn-on transient.

The SiC diode has a small reverse recovery current, which drastically reduces the losses. At high temperature (T_j = 125°C) it presents a softer behavior with reduced ringing and larger losses (10 mJ at T_j = 25°C and 72 mJ at T_j = 125°C). The Si diode, on the other hand, has a high reverse recovery current maximum and losses (0.75 J at T_j = 25°C and 1.75 J at T_j = 125°C).

The reduction of the reverse recovery current peak reduces also the stress and losses of the IGBT during the turn-on transient. With the application of the SiC diode, the peak current was reduced from 1.69 kA to 1.19 kA and the IGBT turn-on losses at 125°C from 11.2 J to 5.7 J. The commutation losses for both diode and IGBT were extracted from the measurements, the results can be seen in Fig. 10. SiC technology offers very low losses and an almost temperature independent behavior.

IV. Converter Loss Estimation

In order to assess the advantages of the SiC diode in a medium voltage converter, a 3L-NPC voltage source converter (VSC) was simulated. Out of the device characterization for the SiC and Si diode, thermal loss models were elaborated. The loss models are coupled to the electrical simulation of the inverter using the software PLECS. For every electrothermal loss model, static and switching losses were extracted for three temperatures (25, 75, 125 °C) throughout the entire device current range.

A. Design

One phase-leg of the simulated converter is shown in Fig.11. The devices are divided in three groups: outer devices T_{out} and

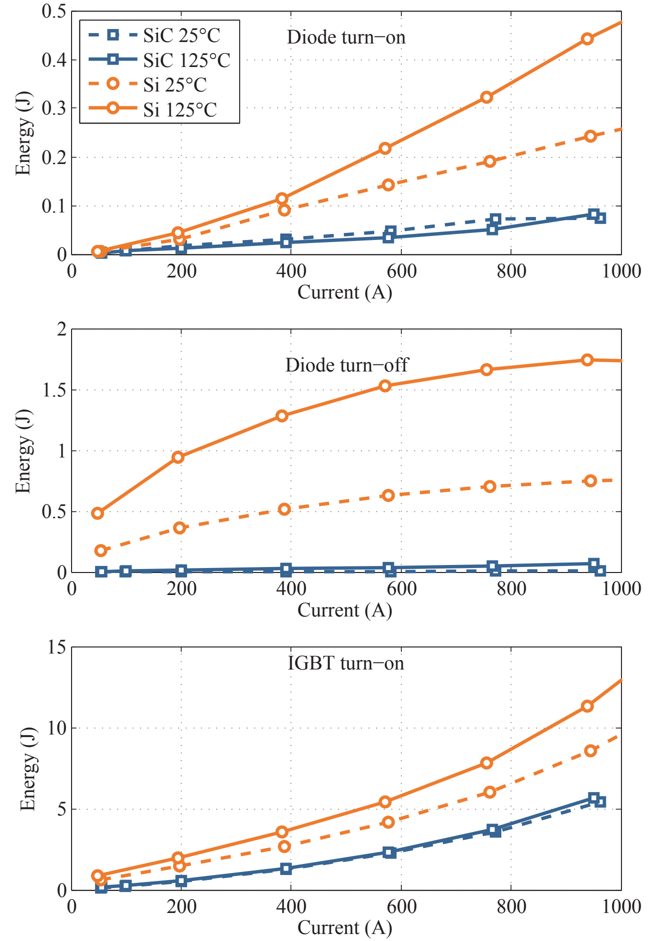

Fig. 10. Switching losses at V_{dc} = 3 kV and I_D = 50. . . 1000 A, di/dt = 1.6 kA/μs at T_j = 25°C and 1.8 kA/μs at 125°C for I_D = 1 kA, IGBT FZ600R65KF2 and Si diode module DD600S65K1 (full).

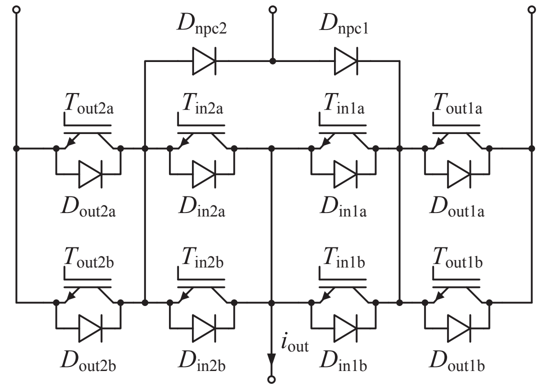

Fig. 11. Phase-leg of the simulated 3L-NPC converter with paralleled modules.

D_{out}, inner devices T_{in} and D_{in} and NPC diodes D_{npc}. With paralleled devices as shown in the picture, an output power of around 6. . . 7 MVA can be achieved.

Three different semiconductor configurations were simulated, see Tab. II. The *All-Si* setup is a full Si based design with commercial devices. For *SiC-NPC*, SiC diodes were

TABLE II
SEMICONDUCTOR DEVICE SETUP FOR CONVERTER SIMULATION

Setup	All-Si	SiC-NPC	SiC-diodes
T_{out}, T_{in}	FZ600R65KF2	FZ600R65KF2	FZ600R65KF2
D_{in}	FZ600R65KF2	FZ600R65KF2	FZ600R65KF2
D_{out}	FZ600R65KF2	FZ600R65KF2	SIC-D40
D_{npc}	DD600S65K1	SiC-D120	SIC-D120

TABLE III
CONVERTER SPECIFICATIONS

DC-link voltage	6,2 kV
Switching frequency	465 Hz
Output frequency	50 Hz
Output voltage	4160 V
Ambient temperature	50 °C
Max. junction temperature	120 °C
Min. IGBT on-time	100 µs

used as NPC diodes. The *SiC-diodes* configuration includes SiC diodes for D_{out} and D_{npc} positions. D_{in} diodes are left in conventional Si technology on purpose, as these diodes do not experience reverse recovery losses, so no advantage is achieved by replacing them with SiC diodes. A similar approach to the *SiC-diodes* configuration can be found in [26].

The IGBT used is a FZ600R65KF2, with nominal ratings of 6.5 kV and 600 A. The Si NPC diode is a DD600S65K1 and contains two 6.5 kV, 600 A diodes. For the simulation, each D_{npc} used a full module (1.2 kA). Regarding the switching speed, the standard gate resistance values for Si devices were kept in the three setups, i.e. $R_{g,on}$ = 4.1 Ω and $R_{g,off}$ = 5.8 Ω. As demonstrated in Fig. 6, further loss reduction could be achieved with lower gate resistance values for the *SiC-diodes* configuration.

In the case of the SiC diode, "SiC-D120" is a 130×190 mm^2 module containing 120 dies. The corresponding loss model was scaled from the characterization of the 80-dies module. Thermal resistances of the SiC prototype were estimated through simulation of the module structure, with a total of $R_{th,jh}$ = 19.9 mW/K for the "SiC-D120" module. Accordingly, "SiC-D40" is a diode with 40 dies and represents a SiC free-wheeling diode (FWD) for the FZ600R65KF2 module. The number of paralleled dies was set to 40 because of space limitations inside the module (1/3 of the total module size). For the cooling, a water-cooled heat sink was modeled, with a thermal resistance of $R_{h,ha}$ = 15 mW/K for a 130×190 mm^2 module.

For the modulation, a sine-triangle PWM with third harmonic injection was chosen, allowing a maximal modulation depth m_a of 1.15. Since the desired output voltage is 4160 V, a dc-link voltage of 2×3088 V was set (5% reserve). For low modulation depths, the reference was alternated from the upper to the lower carrier band (two-level modulation), to avoid overheating of the D_{npc} diodes [27]. A summary of the inverter design parameters can be found in Tab. III.

3L-NPC converters have an unequal temperature distribution among their devices. The four most critical operating points (OP) are at maximum or minimum modulation depth,

TABLE IV
CRITICAL OPERATING POINTS FOR 3L-NPC VSC

	OP1	OP2	OP3	OP4
m_a	max. (1.15)	max (1.15)	min. (0.01)	min. (0.01)
$\cos\varphi$	1 (mot.)	−1 (gen.)	1 (mot.)	−1 (gen.)

TABLE V
MAXIMUM OUTPUT CURRENT FOR EACH OP, f_{SW} = 465 Hz (A)

Set	OP1	OP2	OP3	OP4
All-Si	**828 A**	1030 A	1123 A	1126 A
SiC-NPC	**964 A**	1030 A	1093 A	1127 A
SiC-diodes	**964 A**	1097 A	1218 A	1222 A

and at power factors of 1 or -1, as indicated in [28] and summarized in Tab. IV.

For each critical point, one device position (*in*, *out* or *npc*) per phase-leg has the highest temperature. The maximum current output for a given semiconductor setup is determined by the maximum allowable junction temperature $T_{j,max}$ at the most critical OP. The maximum output current for each critical OP is listed in Tab. V. It can be concluded that for all the configurations studied, OP1 is the most critical and limits the converter. Tab. VI indicates the maximum output power for each configuration.

The results show that the converter power output can be increased in 16% by the use of SiC NPC diodes. By doing so, the outer IGBTs T_{out} turn-on losses are reduced and, thus, a higher output current can be achieved. Changing the outer devices D_{out} to SiC diodes does not translate in additional output power, since the limiting device position T_{out} is not influenced by them.

For some applications, it might be more attractive to increase the switching frequency of the converter, reducing filter size and cost. Using the same methodology explained before, the maximum switching frequency for a given output current and max. junction temperature can be calculated. The results can be found in Tab. VII. With SiC NPC diodes, the switching frequency can be increased in 45%. If we assume that the inductance is inversely proportional to the switching frequency, and that the energy of the inductor is directly proportional to its size, then the size of filter inductor can be reduced in 31%.

B. Efficiency

The three semiconductor configurations were evaluated regarding the overall inverter efficiency. Only semiconductor

TABLE VI
SIMULATION RESULTS FOR MAX. CONVERTER OUTPUT POWER (f_{SW} = 465 Hz)

Set	I_{out}	S_{out}		Lim. device
All-Si	828 A	5.97 MVA	**100%**	T_{in} (OP1)
SiC-NPC	964 A	6.95 MVA	**116%**	T_{in} (OP1)
SiC-diodes	964 A	6.95 MVA	**116%**	T_{in} (OP1)

TABLE VII
SIMULATION RESULTS FOR MAX. SWITCHING FREQUENCY (I_{OUT} = 869 A)

Set	Switching freq. f_{sw}		Size factor ($\propto 1/f_{sw}$)
All-Si	465 Hz	100%	1.00
SiC-NPC	674 Hz	145%	0.69
SiC-diodes	679 Hz	146%	0.68

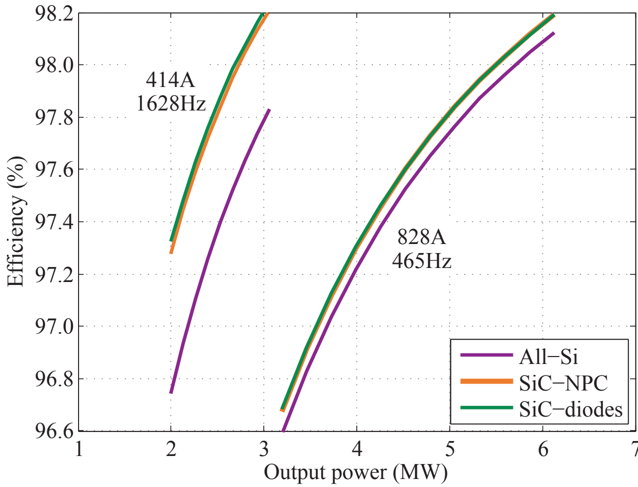

Fig. 12. Efficiency of the 3L-NPC VSI for the three device configurations and two I_{out}, f_{sw} combinations: 828 A, 465 Hz and 414 A, 1628 Hz (V_{dc} = 6.2 kV, $\cos\varphi$= 0.85).

losses, i.e. conduction and switching losses, were considered. The results are shown in Fig. 12 and consider equal load current I_{out} and $\cos\varphi$ of 0.85 for the three cases.

Two scenarios were considered for the analysis: (A) I_{out} = 828 A, f_{sw} = 465 Hz (normal *All-Si* operating conditions), and (B) I_{out}= 0.5×828 A, f_{sw} = 3.5×465 Hz. The second scenario allows to see the advantages of the SiC diodes when operating at higher switching frequencies.

In scenario (A), the SiC diodes do not contribute considerably to a higher efficiency; the improvement is marginal, roughly 0.1% higher. In terms of total semiconductor losses, this amounts to a reduction of 3. . . 4% for the SiC configurations. This is manly related to the high conduction losses of the SiC diode prototype and the relatively low f_{sw} chosen. Both SiC configurations *SiC-NPC* and *SiC-diodes* do not differentiate from each other in the plot, since the extra SiC diodes D_{out} in the *SiC-diodes* configuration are not critical at the $\cos\varphi$ studied. However, even if the efficiency improvement is small, the main advantage of applying SiC diodes under these operating conditions lies in the possibility to increase the converter output power or frequency.

In the case of scenario (B), the advantages of SiC diodes as low switching loss devices become evident. The efficiency can be increased between 0.4 and 0.6% for the plotted power range. The semiconductor losses are reduced in 18. . . 19%. As expected, SiC diodes perform better in applications where the switching frequency is high.

C. Loss analysis

For a better understanding of the loss distribution among the different semiconductors and critical OPs, Fig. 13 was elaborated. The loss distribution for each semiconductor configuration in OP1 and OP2 is plotted, subdivided in conduction and switching losses (Figs. 13a and 13b). Each loss plot is accompanied by the corresponding junction temperature plot (Figs. 13c and 13d).

The effect of SiC diodes as D_{npc} devices can be clearly appreciated. The switching losses are almost zero, see Fig. 13a, but the conduction losses increase. Nonetheless, D_{npc} losses are low compared to the other devices in the inverter and do not limit the inverter power output. As pointed out in [28], the overrating of the D_{npc} diodes is useful in the case of zero speed, where the inverter has an output frequency close to zero. In this operating point, the devices are stressed with the peak value of the load current for a long time.

The most important effect of SiC NPC diodes can be seen in the outer IGBTs T_{out}. These have lower turn-on losses because of the reduced reverse recovery peak of the NPC diode. This is the main reason for the higher power output and efficiency, see Fig. 13a T_{out}. In terms of junction temperature, this translates into 12°C less for T_{out} operating with SiC NPC diodes.

Taking a closer look at the *SiC-diodes* configuration, Figs. 13b and 13d D_{out}, the effects of a higher thermal resistance $R_{th,jc}$ and $R_{th,ch}$ for the SiC diode can be appreciated (24% higher than the antiparallel Si diode). When using antiparallel SiC diodes, the area available inside the module is limited to one third of the total module surface. This limits the number of paralleled diode chips to 40 pieces. Thus, despite the loss reduction achieved by the SiC diode, its junction temperature is higher.

D. Summary

Through the use of this thermoelectrical simulation model an estimation of the extra power output of a 3L-NPC inverter could be made. With the replacement of the common Si NPC diodes by SiC technology in the analyzed converter, an increase in output power of 16% can be achieved. It was demonstrated that the reduction of the turn-on losses in the outer IGBTs is the main advantage of applying SiC NPC diodes. An additional replacement of the outer Si diodes by SiC diodes has no influence in the maximum output power, as this extra diodes do not have influence on the losses of the limiting device T_{out}.

It is important to note that the comparison did not consider increasing the di/dt during IGBT turn-on when using SiC diodes. Through this measure, an additional increase of output current / switching frequency can be achieved. A future publication will analyze further alternatives that would allow to go over the 16% extra output power calculated here.

V. CONCLUSIONS

This paper has presented an overview of the new 6.5-kV, 1-kA SiC diode module prototype, including a comparison on device level with a commercial Si diode and evaluation of

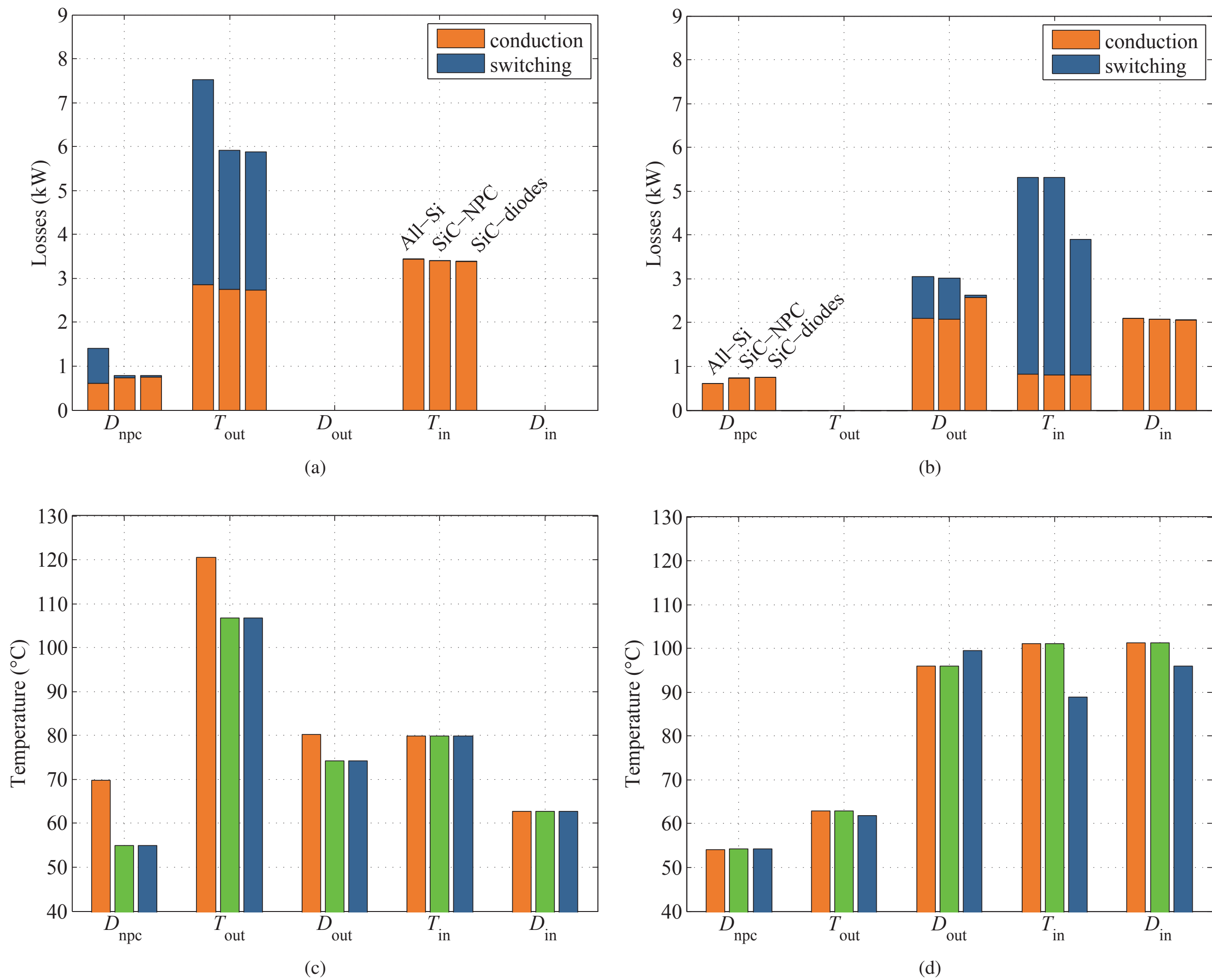

Fig. 13. Conduction and switching losses for OP1 (a) and OP2 (b) for the three semiconductor setups per one phase-leg. Each column represents the losses of one device group, e.g. each T_{out} bar accounts for the total losses of T_{out1a}, T_{out1b}, T_{out2a} and T_{out2b}. Junction temperature of each device group for OP1 (c) and OP2 (d). (V_{dc} = 6.2 kV, I_{out} = 828 A, f_{sw} = 465 Hz)

this technology when applied in a 3L-NPC VSC through an electrothermal simulation model.

The prototype is able to switch the desired current (1000 A per module) successfully. The forward characteristic exhibits a higher on-state voltage than the Si counterpart. The SiC diode properties do not have a strong temperature dependency, in contrast to Si diodes.

The switching behavior has still some issues regarding ringing, which can be solved by correctly dimensioning an RC snubber [24]. The diode offers marginal losses with low device stress. Further reduction can be achieved by increasing the di/dt through the IGBT gate resistor, as the reverse recovery peak is not limiting factor in SiC diodes. The reduction of losses in the IGBT by the inclusion of a SiC freewheeling diode was also demonstrated, which amount to 50% for the turn-on transient at 125°C.

The reduction of semiconductor losses through the use of SiC devices will allow a higher power output for converters without increasing their size, or a reduction of the filter size in case a switching frequency increase is preferred. Based on the simulations here presented, an increase of the output power of 16% for a 6-MVA 3L-NPC VSC is expected, when using SiC technology for the NPC diodes. Alternatively, the switching frequency could be increased in 46%. These calculations do not consider extra adjustments, such as increasing the di/dt during IGBT turn-on, which would allow to go beyond these values.

Acknowledgment

This work was financially supported by the German Federal Ministry of Education and Research (BMBF).

References

[1] Q. Zhang, R. Callanan, M. Das, S.-H. Ryu, A. Agarwal, and J. Palmour, “SiC power devices for microgrids,” *IEEE Trans. Power Electron.*, vol. 25, no. 12, pp. 2889–2896, Dec. 2010.

[2] J. Rabkowski, D. Peftitsis, and H. Nee, “Silicon carbide power transistors: A new era in power electronics is initiated,” *IEEE Ind. Electron. Mag.*, vol. 6, no. 2, pp. 17–26, Jun. 2012.

[3] G. Miller, “New semiconductor technologies challenge package and system setups,” in *Proc. 6th Int. Integrated Power Electronics Systems (CIPS) Conf.*, March 2010.

[4] M. Treu, R. Rupp, and G. Solkner, “Reliability of SiC power devices and its influence on their commercialization – review, status, and remaining issues,” in *Reliability Physics Symposium (IRPS), 2010 IEEE Int.* IEEE, May 2010, pp. 156–161.

[5] P. Friedrichs, “SiC power devices for industrial applications,” in *Proc. Int. Power Electronics Conf. (IPEC)*. IEEE, Jun. 2010, pp. 3241–3248.

[6] L. Cheng, A. K. Agarwal, M. O’Loughlin, C. Capell, K. Lam, C. Jonas, J. Richmond, A. Burk, J. W. Palmour, A. A. Ogunniyi, H. K. O’Brien, and C. J. Scozzie, “16 kV, 1 cm^2, 4H-SiC PiN diodes for advanced high-power and high-temperature applications,” in *Materials Science Forum*, vol. 740–742. Trans Tech Publ, Jan. 2013, pp. 895–898.

[7] S.-H. Ryu, C. Capell, C. Jonas, L. Cheng, M. O’Loughlin, A. Burk, A. Agarwal, J. Palmour, and A. Hefner, “Ultra high voltage (>12 kV), high performance 4H-SiC IGBTs,” in *Proc. 24th Int. Symp. Power Semiconductor Devices and ICs ISPSD ’12*, 2012, pp. 257–260.

[8] S. G. Sundaresan, C. Sturdevant, M. Marripelly, E. Lieser, and R. Singh, “12.9 kV SiC PiN diodes with low on-state drops and high carrier lifetimes,” in *Materials Science Forum*, vol. 717–720. Trans Tech Publ, May 2012, pp. 949–952.

[9] K. Takao, K. Wada, K. Sung, Y. Mastuoka, Y. Tanaka, S. Nishizawa, C. Ota, T. Kanai, T. Shinohe, and H. Ohashi, “4.5kV-400A modules using SiC-PiN diodes and Si-IEGTs hybrid pair for high power medium-voltage power converters,” in *IEEE Energy Conversion Congress and Exposition, ECCE 2012*. IEEE, Sep. 2012, pp. 1509–1514.

[10] A. Tanaka, S. Ogata, T. Izumi, K. Nakayama, T. Hayashi, Y. Miyanagi, and K. Asano, “Reliability investigation of SiC bipolar device module in long time inverter operation,” in *Proc. 24th Int. Symp. Power Semiconductor Devices and ICs ISPSD ’12*, 2012, pp. 233–236.

[11] A. Elasser, M. Agamy, J. Nasadoski, A. Bolotnikov, Z. Stum, R. Raju, L. Stevanovic, J. Mari, M. Menzel, B. Bastien, and P. Losee, “Static and dynamic characterization of 6.5kV, 100A SiC bipolar PiN diode modules,” in *IEEE Energy Conversion Congress and Exposition, ECCE 2012*. IEEE, Sep. 2012, pp. 3595–3602.

[12] M. K. Das, C. Capell, D. E. Grider, R. Raju, M. Schutten, J. Nasadoski, S. Leslie, J. Ostop, and A. Hefner, “10 kV, 120 A SiC half H-bridge power MOSFET modules suitable for high frequency, medium voltage applications,” in *IEEE Energy Conversion Congress and Exposition, ECCE 2011*. IEEE, Sep. 2011, pp. 2689–2692.

[13] Y. Sugawara, S. Ogata, S. Okada, T. Izumi, Y. Miyanagi, K. Asano, K. Nakayama, and A. Tanaka, “4.5 kV 1000 A class SiC pn diode modules with resin mold package and ceramic flat package,” in *Proc. 20th Int. Symp. Power Semiconductor Devices and ICs ISPSD ’08*, May 2008, pp. 267–270.

[14] F. Filsecker, R. Alvarez, and S. Bernet, “Characterization of a new 6.5 kV 1000A SiC diode for medium voltage converters,” in *IEEE Energy Conversion Congress and Exposition, ECCE 2012*. Raleigh, USA: IEEE, Sep. 2012, pp. 2253–2260.

[15] ——, “Comparison of 6.5 kV silicon and SiC diodes,” in *IEEE Energy Conversion Congress and Exposition, ECCE 2012*. Raleigh, USA: IEEE, Sep. 2012, pp. 2261–2267.

[16] D. Peters, W. Bartsch, B. Thomas, and R. Sommer, “6.5 kV SiC PiN diodes with improved forward characteristics,” in *Materials Science Forum*, vol. 645–648. Trans Tech Publ, Apr. 2010, pp. 901–904.

[17] D. Peters, B. Thomas, T. Duetemeyer, T. Hunger, and R. Sommer, “An experimental study of high voltage SiC PiN diode modules designed for 6.5 kV / 1 kA,” in *Materials Science Forum*, vol. 679-680. Trans Tech Publ, Mar. 2011, pp. 531–534.

[18] R. Singh, “Reliability and performance limitations in SiC power devices,” *Microelectronics Reliability*, vol. 46, no. 5–6, pp. 713–730, 2006.

[19] N. Kondrath and M. Kazimierczuk, “Characteristics and applications of silicon carbide power devices in power electronics,” *International Journal of Electronics and Telecommunications*, vol. 56, no. 3, pp. 231–236, Jan. 2010.

[20] J.-H. Fabian, S. Hartmann, and A. Hamidi, “Analysis of insulation failure modes in high power IGBT modules,” in *Industry Applications Conference, 2005. Fourtieth IAS Annual Meeting. Conference Record of the 2005*, vol. 2. IEEE, Oct. 2005, pp. 799–805.

[21] R. Wang, D. Boroyevich, P. Ning, Z. Wang, F. Wang, P. Mattavelli, K. D. T. Ngo, and K. Rajashekara, “A high-temperature SiC three-phase AC–DC converter design for 100C ambient temperature,” *IEEE Trans. Power Electron.*, vol. 28, no. 1, pp. 555–572, 2012.

[22] K. Dohnke, W. Bartsch, R. Schörner, and T. Van Weelden, “A molded package optimized for high voltage SiC-devices,” in *Materials Science Forum*, vol. 679–680. Trans Tech Publ, Mar. 2011, pp. 762–765.

[23] I. Josifovic, J. Popovic-Gerber, and J. Ferreira, “Improving SiC JFET switching behavior under influence of circuit parasitics,” *IEEE Trans. Power Electron.*, vol. 27, no. 8, pp. 3843–3854, Aug. 2012.

[24] F. Filsecker, R. Alvarez, and S. Bernet, “Investigation of oscillations in a 6.5-kV, 1-kA SiC diode module,” in *Proc. 15th European Conf. on Power Electronics and Applications EPE’13 ECCE Europe*, 2013.

[25] M. Rahimo and N. Shammas, “Freewheeling diode reverse-recovery failure modes in IGBT applications,” *IEEE Trans. Ind. Appl.*, vol. 37, no. 2, pp. 661–670, Mar./Apr. 2001.

[26] M. Schweizer, T. Friedli, and J. Kolar, “Comparison and implementation of a 3-level NPC voltage link back-to-back converter with SiC and Si diodes,” in *Proc. IEEE Applied Power Electronics Conf. and Exposition APEC 2010*, Feb. 2010, pp. 1527–1533.

[27] T. Brückner and D. G. Holmes, “Optimal pulse-width modulation for three-level inverters,” *IEEE Trans. Power Electron.*, vol. 20, no. 1, pp. 82–89, Jan. 2005.

[28] T. Brückner and S. Bernet, “Loss balancing in three-level voltage source inverters applying active NPC switches,” in *Proc. IEEE Power Electronics Specialists Conf. PESC 2001*, vol. 2, 2001, pp. 1135 –1140 vol.2.